NEW FISSION-BARRIER CALCULATION

P. Möller and A. J. Sierk (LANL)

T. Ichikawa (RIKEN)

A. Iwamoto (JAEA)

R. Bengtsson, Henrik Uhrenholt, and Sven Åberg (LUND)

In fission, what are the shapes and related energies involved in the transition from a single ground-state shape to two separated fission fragments?

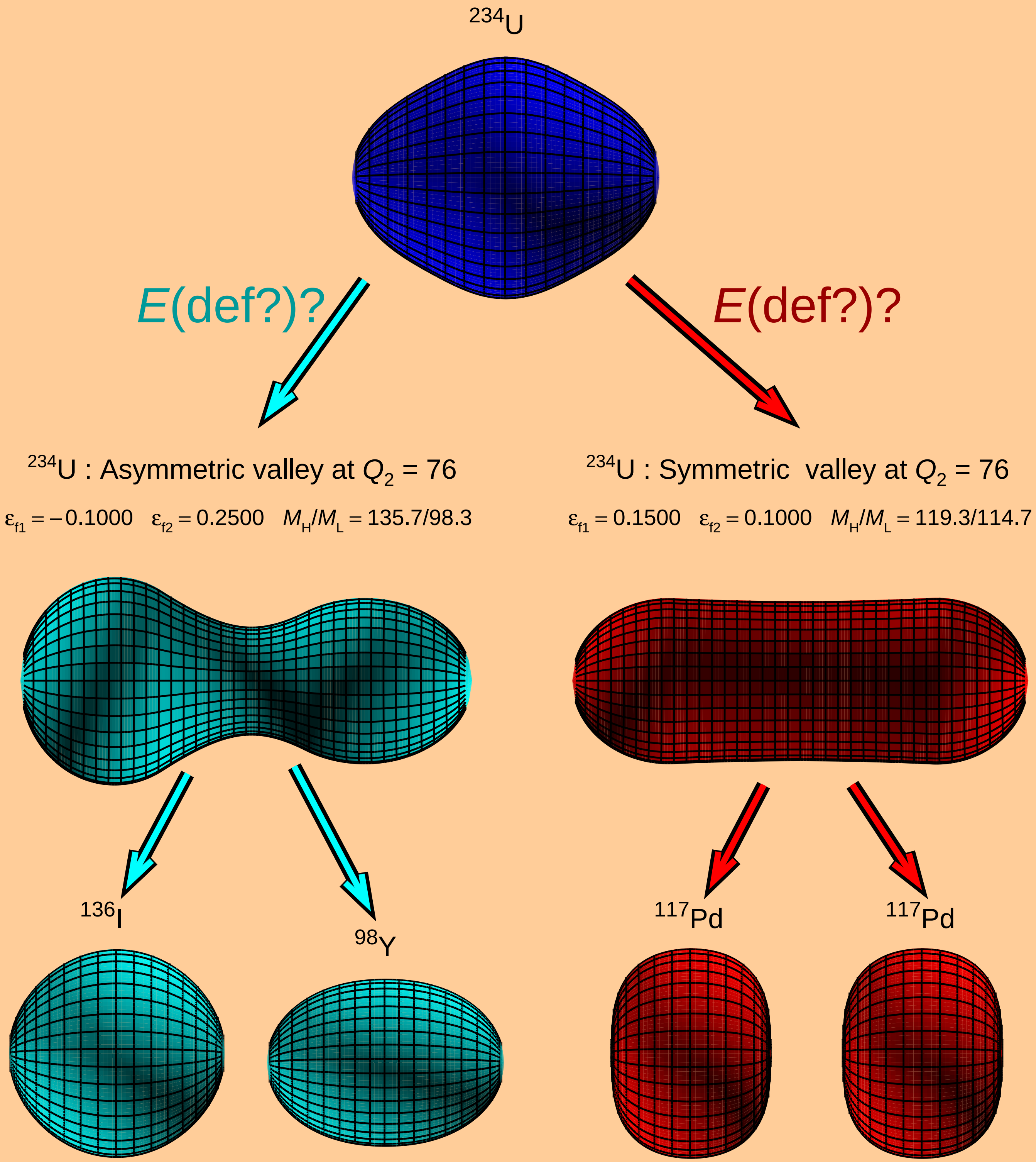

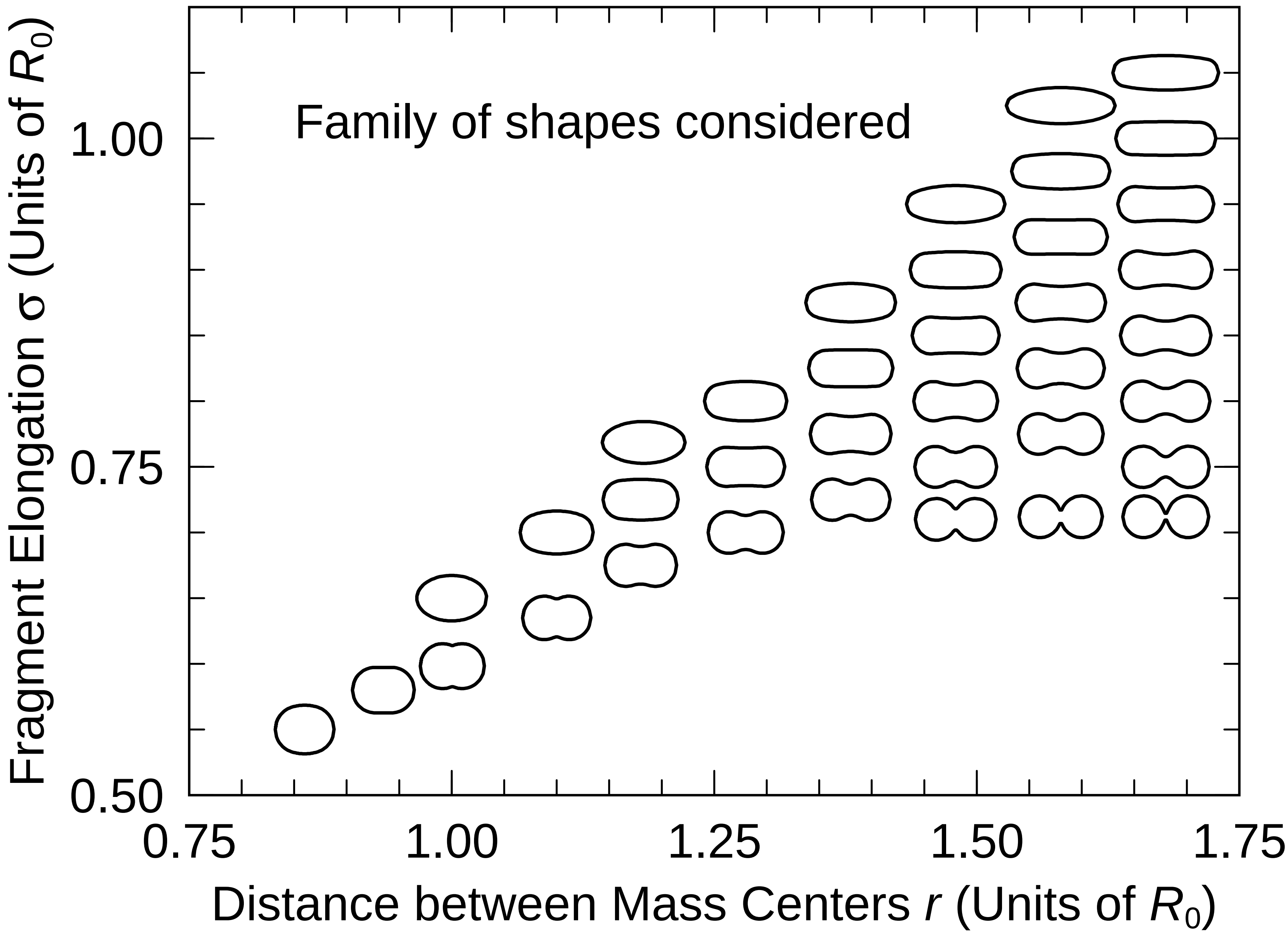

Family of shapes considered
1.00
0.75
0.50
0.75
1.00
1.25
1.50
1.75
Fragment Elongation σ (Units of R_0)
Distance between Mass Centers r (Units of R_0)

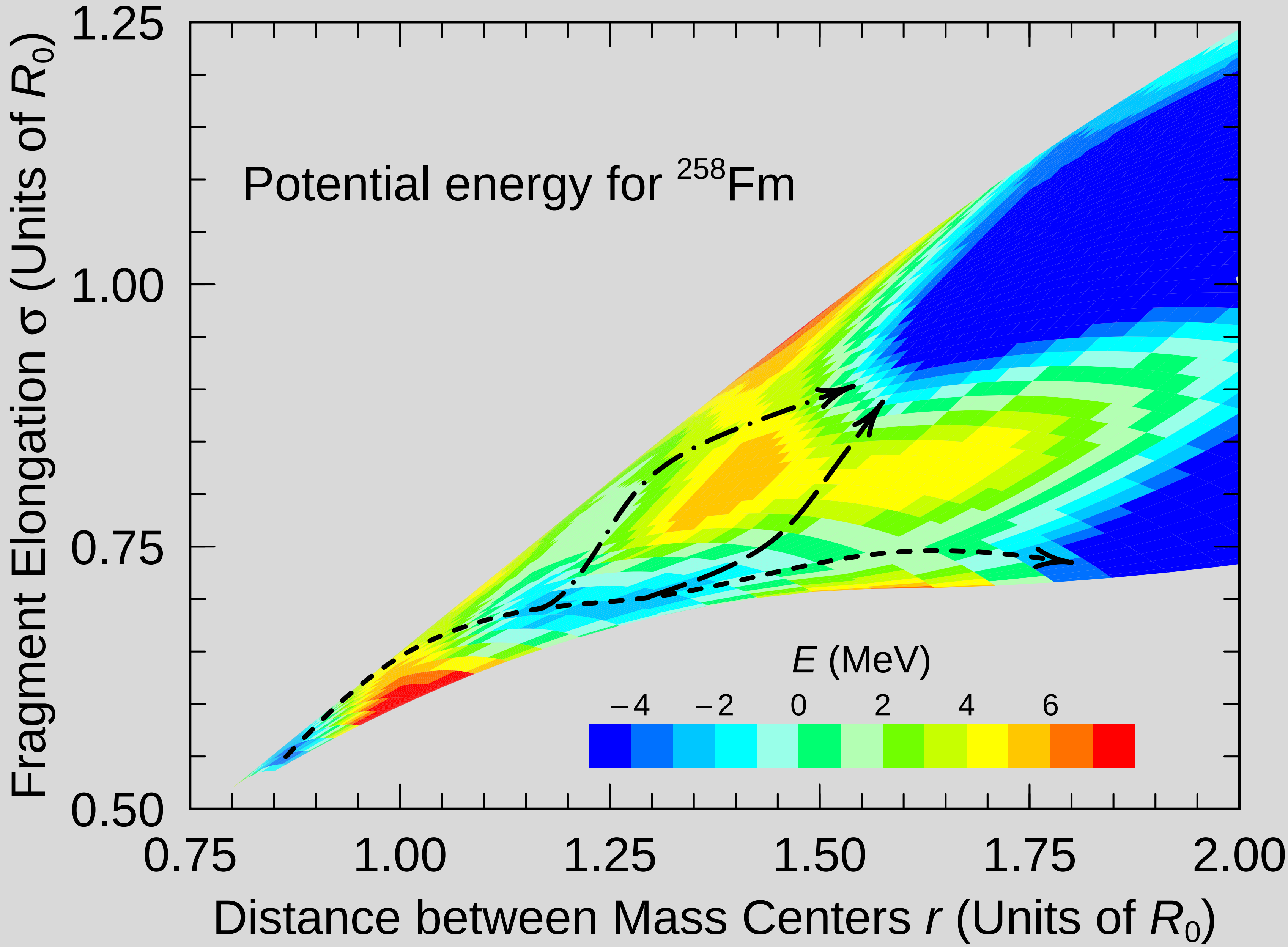

Potential energy for ^{258}Fm
Fragment Elongation σ (Units of R_0)
Distance between Mass Centers r (Units of R_0)
1.25
1.00
0.75
0.50
0.75
1.00
1.25
1.50
1.75
2.00
E (MeV)
−4
−2
0
2
4
6

Five Essential Fission Shape Coordinates

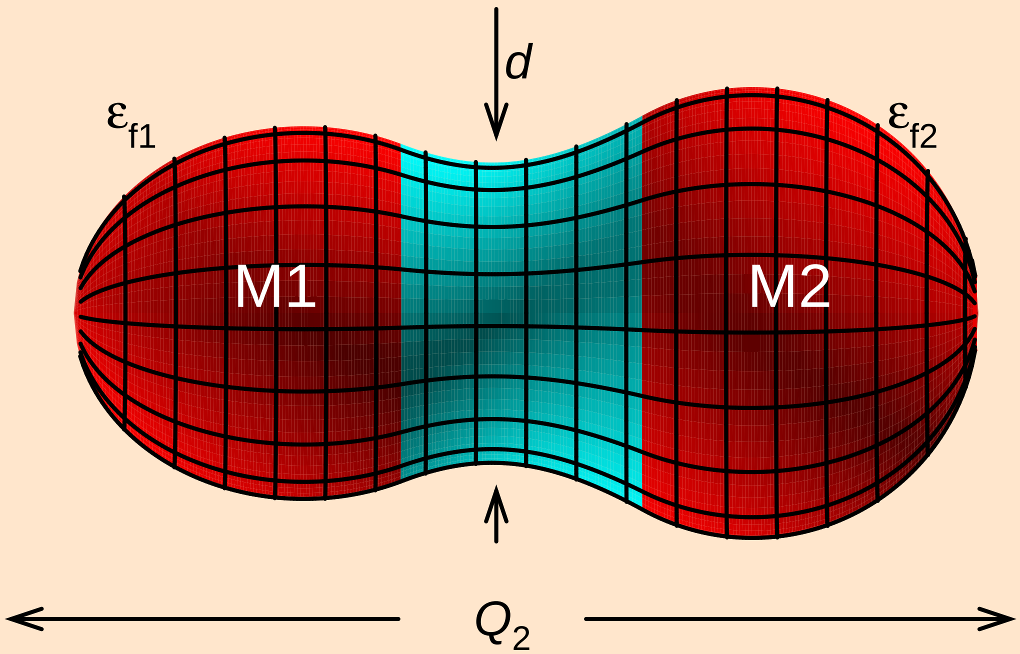

45 Q_2 ~ Elongation (fission direction)

$\otimes$

35 α_g ~ (M1-M2)/(M1+M2) Mass asymmetry

$\otimes$

15 ε_{f1} ~ Left fragment deformation

$\otimes$

15 ε_{f2} ~ Right fragment deformation

$\otimes$

15 d ~ Neck

$\Rightarrow$ 5 315 625 grid points – 306 300 unphysical points

$\Rightarrow$ 5 009 325 physical grid points

1.D.2:
1.E.2

Nuclear Physics **A203** (1973) 433—472; © *North-Holland Publishing Co., Amsterdam*

NUCLEAR DEFORMATION ENERGY CURVES WITH THE CONSTRAINED HARTREE-FOCK METHOD

H. FLOCARD and P. QUENTIN †

Institut de Physique Nucléaire, Division de Physique Théorique, B.P. 1, 91406-Orsay, France ††

and

A. K. KERMAN and D. VAUTHERIN

Laboratory for Nuclear Science and Department of Physics, MIT, Cambridge, Massachusetts †††

Received 20 November 1972

Abstract: Calculations of the deformation energy curves of relatively heavy deformed nuclei – Ce isotopes – have been performed using the constrained Hartree-Fock technique. The two-body interaction is the Skyrme force, and pairing effects are taken into account. Different possible choices for the external field form are investigated and the advantage of a non-linear dependence of the constraint is shown. One of the advantages of this type of calculation is that deformation energy curves can be calculated without making a complete map of the deformation energy surface. A discussion of the numerical techniques and uncertainties, particularly those connected with truncation effects is given. General trends of the deformation energy curves, calculated for the Ce isotopes as a function of the quadrupole moment, are found to be in good agreement with available experimental information. Associated physical quantities are discussed and a comparison is made with the results of phenomenological calculations using the liquid-drop model and the Strutinsky prescription.

1. Introduction

There have been many different attempts to use self-consistent field calculations to determine the properties of nuclei over the past ten years. These have used both purely phenomenological and more fundamental treatments of the two-body force and have examined a large class of different questions ranging from the exact charge density to the quadrupole moments of deformed nuclei.

In this paper we wish to report on a phenomenological self-consistent calculation with the Skyrme interaction [1]) for the energy surfaces of relatively heavy deformed nuclei. Our main aim is not to show that these surfaces are good ones (although they seem to be) but to give a discussion of the various techniques and problems which arise.

The technique used is that of constrained Hartree-Fock (CHF) with pairing and general external field forms. It has been found that the energy surface can be obtained

† Visiteur CEA (D.Ph.T. Saclay).

†† Laboratoire associé au CNRS.

††† This work is supported in part through funds provided by the Atomic Energy Commission under contract AT(II-1)-3069.

March 1973

to the energy surfaces show clearly that for deformations below the saddle point of a heavy nucleus, Q and h are the most important degrees of freedom. These produce axially symmetric shapes with an equatorial symmetry plane. In fact these are the only shapes that our calculations can, up to now, take into account. Degrees of freedom like Y_{30} and $Y_{2\pm 2}$ must be considered eventually if we wish to discuss the fission barrier or nearly spherical nuclei.

Let us suppose that we know the energy surface $E(Q, h)$. When we constrain only Q we follow a path $h^1(Q)$ defined by the equation in the plane (Q, h)

$$\frac{\partial E}{\partial h}(Q, h^1) = 0, \tag{15}$$

and we draw a curve $E^1(Q) = E(Q, h^1(Q))$. On the other hand, if we search for the valley in the plane (Q, h) we get its equation $h^v(Q)$ by solving

$$\frac{dh^v}{dQ}\frac{\partial E(Q, h^v)}{\partial Q} + \frac{\partial E(Q, h^v)}{\partial h} = 0, \tag{16}$$

and the energy curve will be

$$E^v(Q) = E(Q, h^v(Q)). \tag{17}$$

In fig. 2 one can see as an example that h^1 is generally distinct from h^v. It shows that with a single constraint on Q one always gets

$$E^1(Q) \leqq E^v(Q). \tag{18}$$

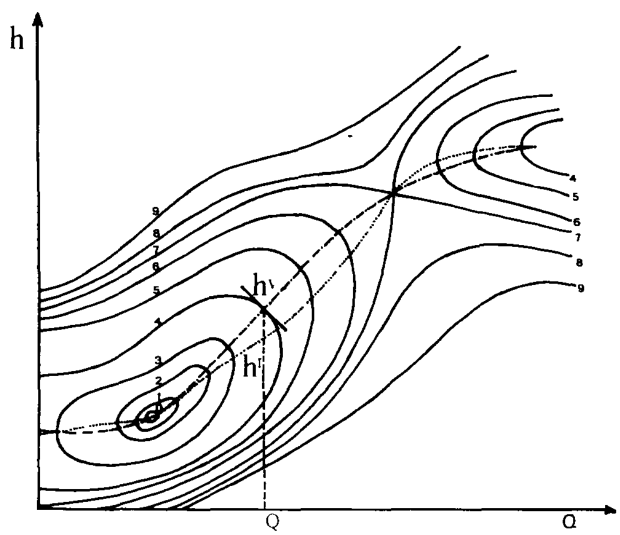

Fig. 2. Example of an energy surface in the (Q, h) plane showing that one does not exactly follow the fission valley with a constraint only on Q.

However, knowledge of $\mathrm{d}h^{\mathrm{v}}/\mathrm{d}Q$ implies knowledge of the fission path. However this can provide an indication on a way to improve the results obtained with a single minimization on Q. We can make a supplementary calculation constraining the quantity

$$P' = Q + h\,\frac{\mathrm{d}h^{1}(Q)}{\mathrm{d}Q}. \tag{21}$$

Within this method one searches for the minimum in a direction perpendicular to the curve h^1 and one comes closer to the true path h^{v}. In fact such a calculation will only be useful if one notices in the curve $h^1(Q)$ a rapid variation showing that the valley becomes rather perpendicular to the Q-axis and consequently that the constraint on Q is not well suited. This method gives a reasonably good approximation to the valley and avoids a complete calculation of the surface $E(Q, h)$. One can also think of using the good approximation given by the liquid-drop model. Indeed one can imagine that the function $h^{\mathrm{LD}}(Q)$ giving the hexadecapole moment of a liquid drop as a function of its quadrupole moment indicates roughly the direction of the valley. In fact phenomenological approaches to deformation energy surfaces show that this is in general true up to the fission saddle point. For future calculations then, it seems also interesting to constrain the quantity

$$P'' = Q + h\,\frac{\mathrm{d}h^{\mathrm{LD}}(Q)}{\mathrm{d}Q}. \tag{22}$$

The point could be made that all this trouble in finding the valley is not really necessary because all we are interested in are the minimum and maximum points, which are correctly given in any case. This is not really so because, in particular for the fission barrier, we would ultimately like to know something about the shape of the curve for dynamical calculations, such as for lifetimes.

However, we do see that it is probably not necessary to calculate the whole energy surface in order to get the information we would like. This is in some contrast to the phenomenological shell-model approaches, which do require an extensive mapping before the valley is identified, with certainty. This point serves to reduce the relative computer time considerably for self-consistent calculations.

2.3. APPROXIMATE TREATMENT OF PAIRING

The single-particle level density in heavy deformed nuclei is large enough so that the question as to which levels near the Fermi level are actually occupied becomes a major source of computational difficulty. In principle one would have to get a separate energy surface for each possible occupation and look at the envelope of these curves. Apart from the problems of computation and the difficulties associated with degeneracies, such a program is really wasted effort because we know that pairing exists in all the deformed nuclei and that the occupation probabilities are determined more or less by the pairing. Partly because of the foregoing and partly because pairing

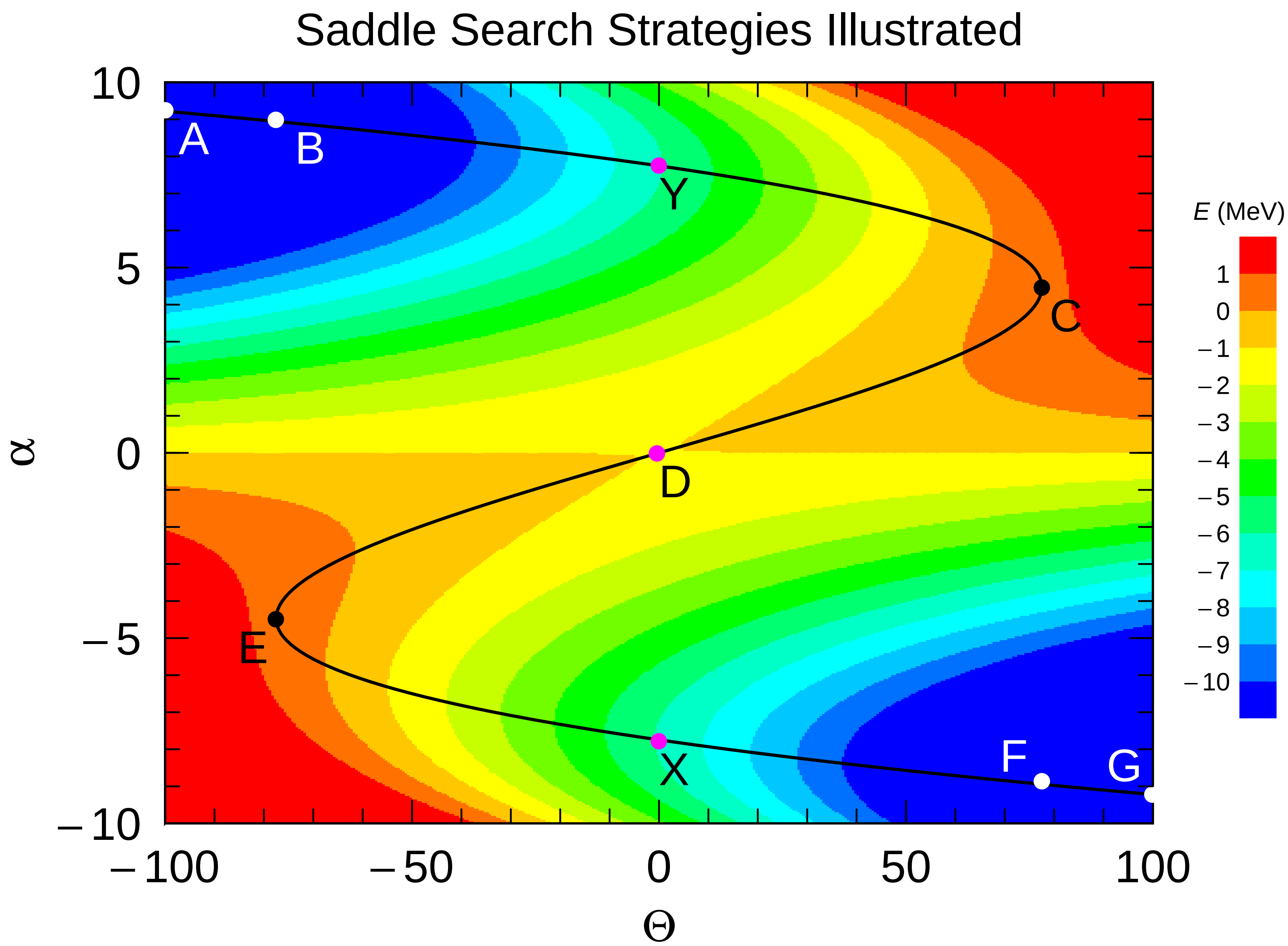
Saddle Search Strategies Illustrated
E (MeV)
1
0
−1
−2
−3
−4
−5
−6
−7
−8
−9
−10
α
Θ
10
5
0
−5
−10
−100
−50
0
50
100
A
B
Y
C
D
E
X
F
G

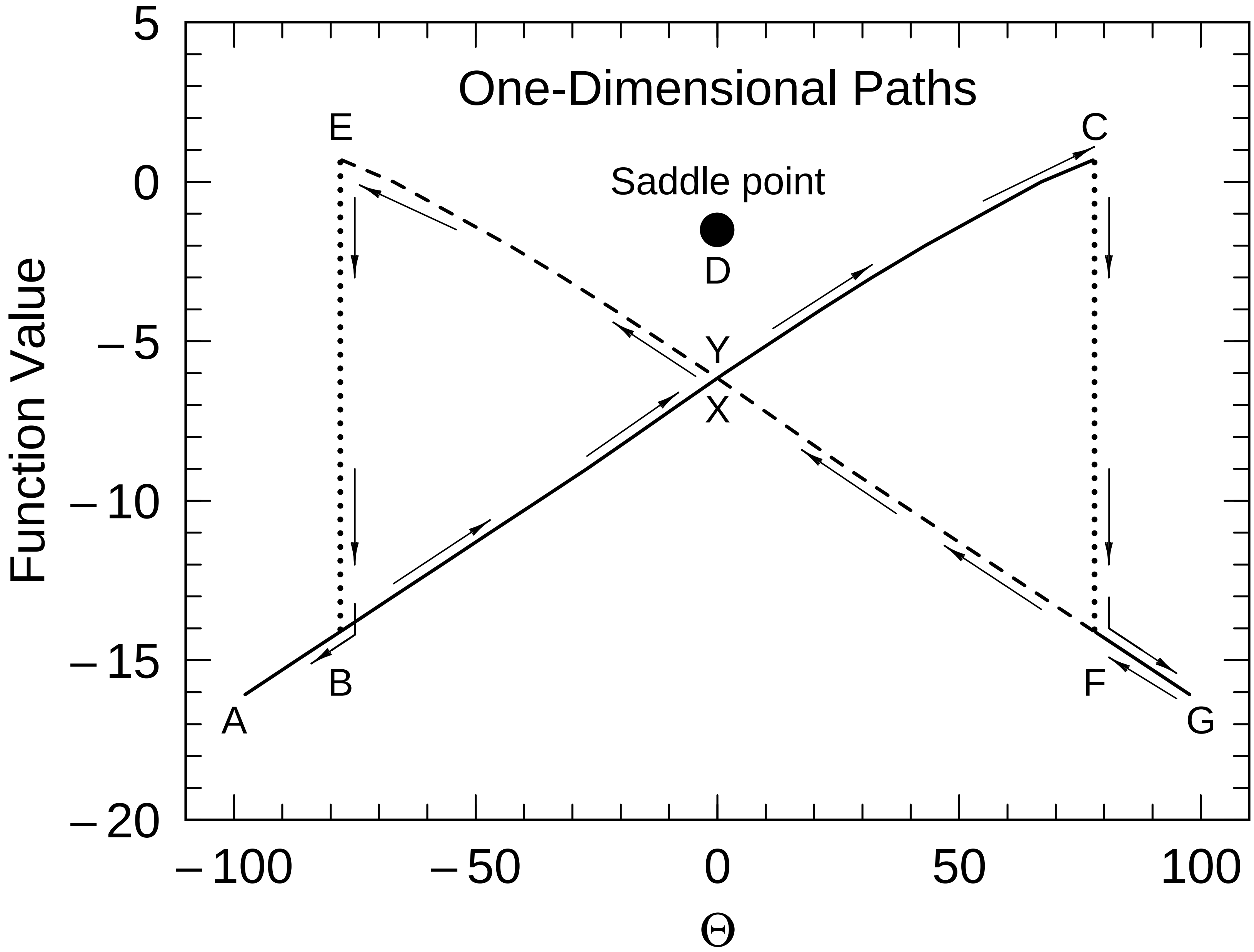

One-Dimensional Paths
Saddle point
Function Value
Θ
5
0
−5
−10
−15
−20
−100
−50
0
50
100
A
B
C
D
E
F
G
X
Y

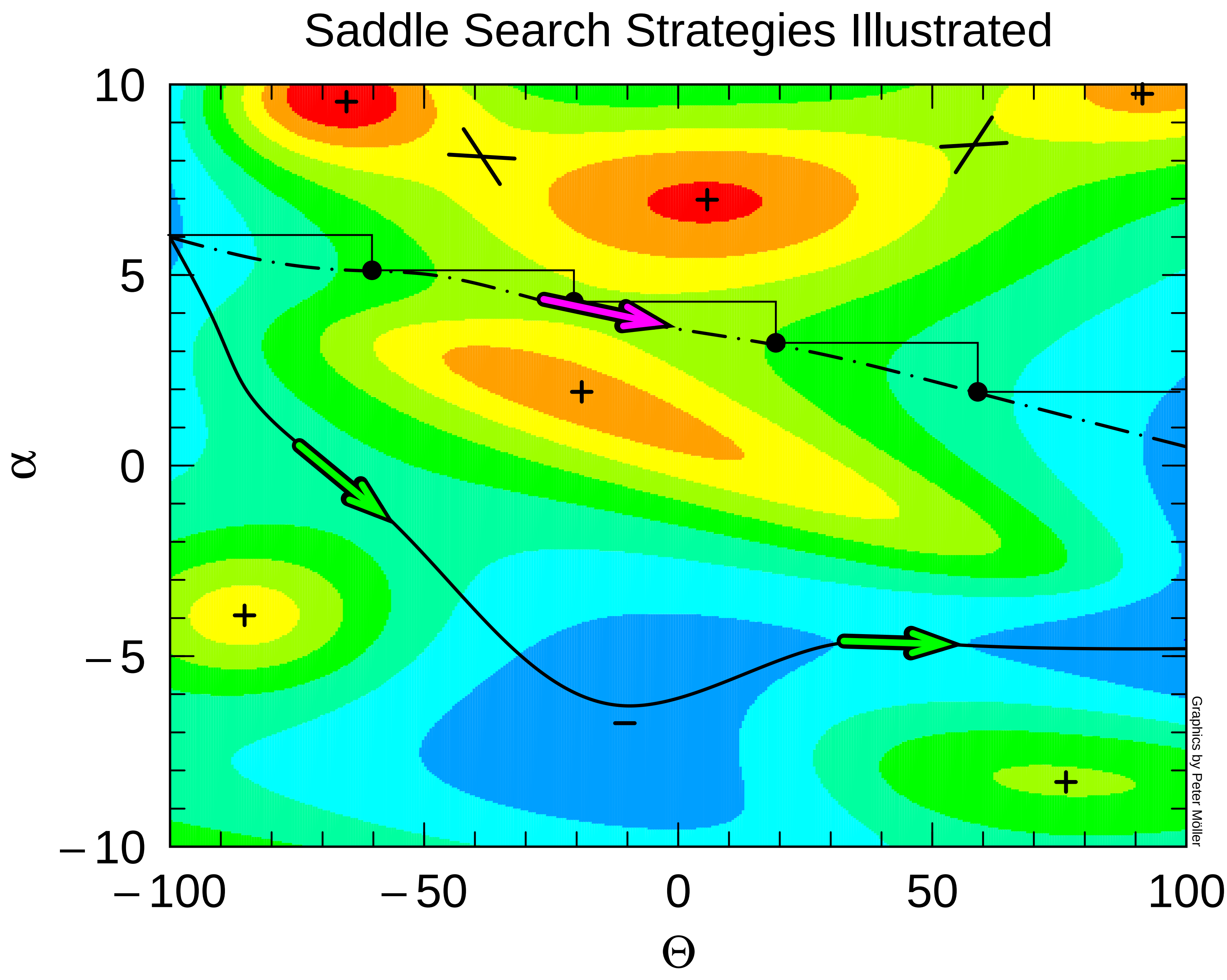
Saddle Search Strategies Illustrated
10
5
0
−5
−10
α
−100
−50
0
50
100
Θ
Graphics by Peter Möller

Potential Energy of Deformation

We use the macroscopic-microscopic method introduced by Swiatecki and Strutinsy:

$$E_{\mathrm{pot}}(\mathrm{shape}) = E_{\mathrm{macr}}(\mathrm{shape}) + E_{\mathrm{micr}}(\mathrm{shape}) \quad (1)$$

The macroscopic term is calculated in a liquid-drop type model (for a specific deformed shape).

The microscopic correction is determined in the following steps

1. A shape is prescribed
2. A single-particle potential with this shape is generated. A spin-orbit term is included.
3. The Schrödinger equation is solved for this deformed potential and single-particle levels and wave-functions are obtained
4. The shell correction is calculated by use of Strutinsky's method.
5. The pairing correction is calculated in the BCS or Lipkin-Nogami method.

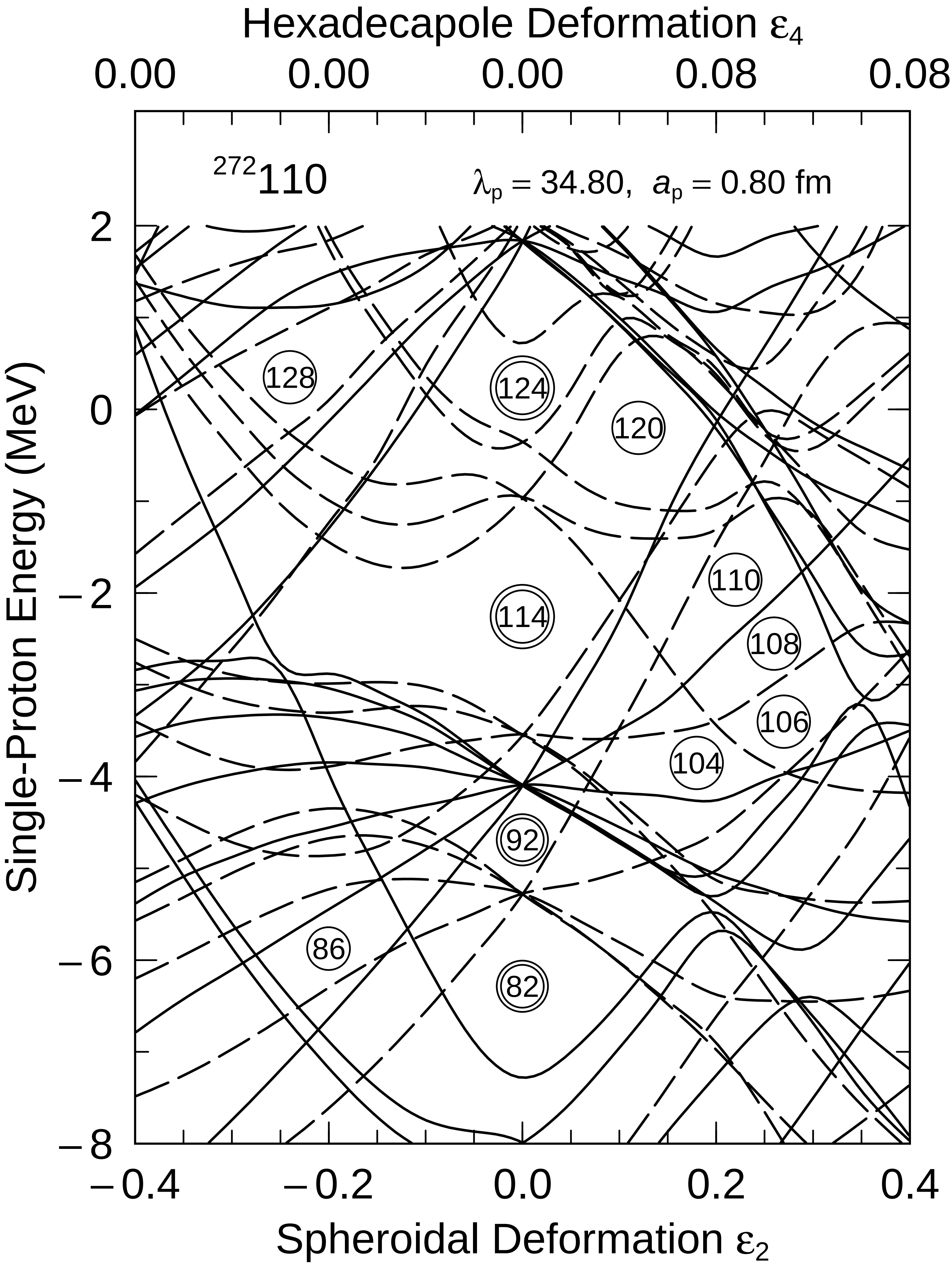

Hexadecapole Deformation ε4
0.00
0.00
0.00
0.08
0.08
272110
λp = 34.80, ap = 0.80 fm
2
0
−2
−4
−6
−8
128
124
120
110
114
108
106
104
92
86
82
Single-Proton Energy (MeV)
−0.4
−0.2
0.0
0.2
0.4
Spheroidal Deformation ε2

Fission Calculation Details

1. Fission Barriers of 5254 nuclei calculated for
   $170 < A \leq 330$
   Several different parameterizations are used
2. 5D parameterization, energy for 5 000 000 different shapes are calculated for each nucleus
3. For small deformations a 3D parameterization is used Elongation, neck and axial-asymmetry shape degrees of freedom.
4. An improved determination of the ground-state energy and shape is done in a 4D space
5. When multiple minima are present a special strategy is used to establish which minimum and saddle define the "barrier".
   (In practice this technique cannot be implemented in HFB)

6. Just the potential energies correspond to more than 250 Gb of information.

7. Saddles, minima, valleys are determined in a completely automated fashion. Compact result files are generated for each nucleus

8. Data sets, such as tables of barrier heights (Z, N, A, E_{f}) are generated, also by automated scripts.

Results will be made available at URL
http://t16web.lanl.gov/Moller/abstracts.html
(Capital M is essential)
Results more complete than can be published will be available here in due course.

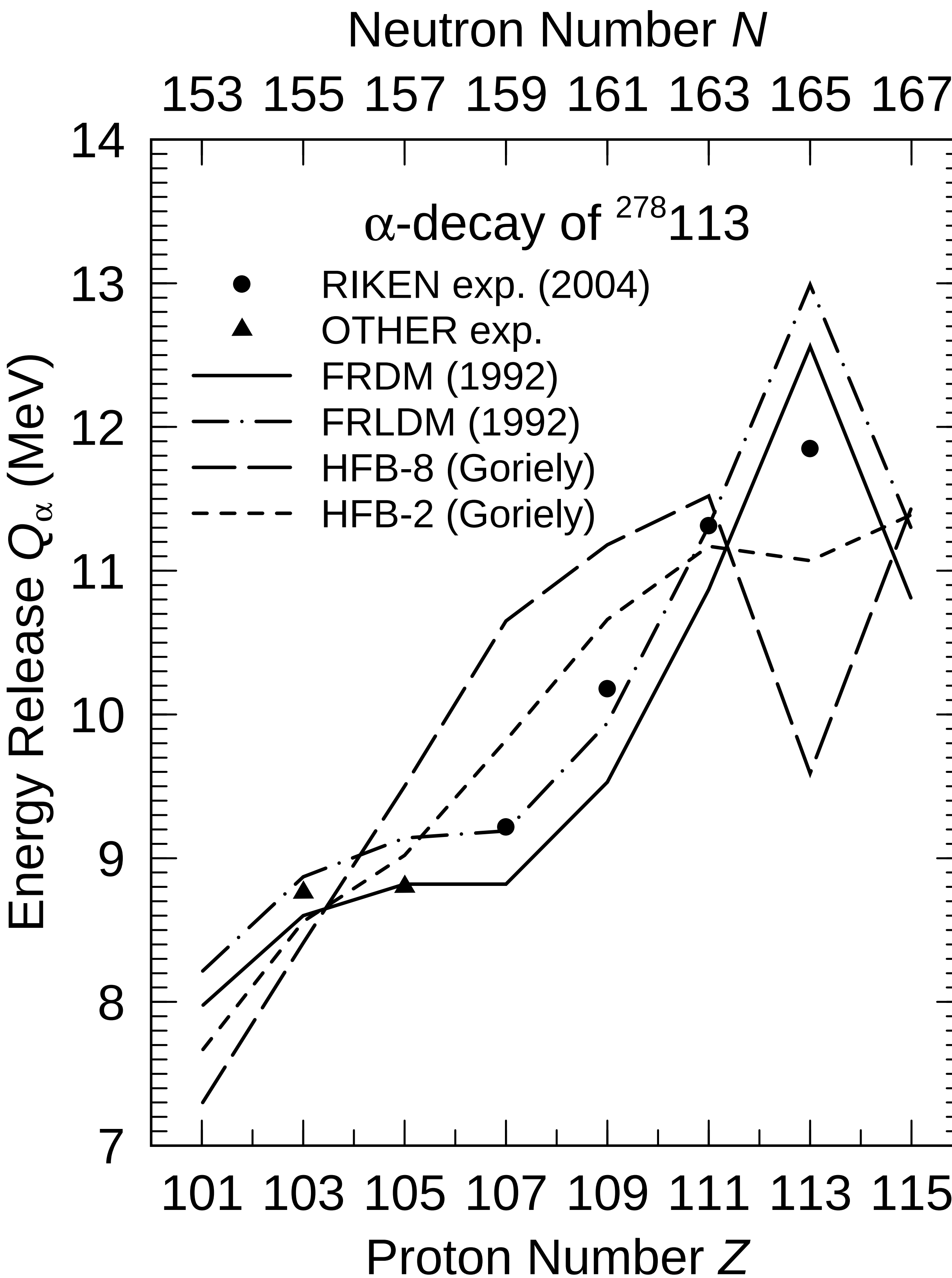

Neutron Number N
153 155 157 159 161 163 165 167
α-decay of 278113
RIKEN exp. (2004)
OTHER exp.
FRDM (1992)
FRLDM (1992)
HFB-8 (Goriely)
HFB-2 (Goriely)
Energy Release Qα (MeV)
14
13
12
11
10
9
8
7
101 103 105 107 109 111 113 115
Proton Number Z

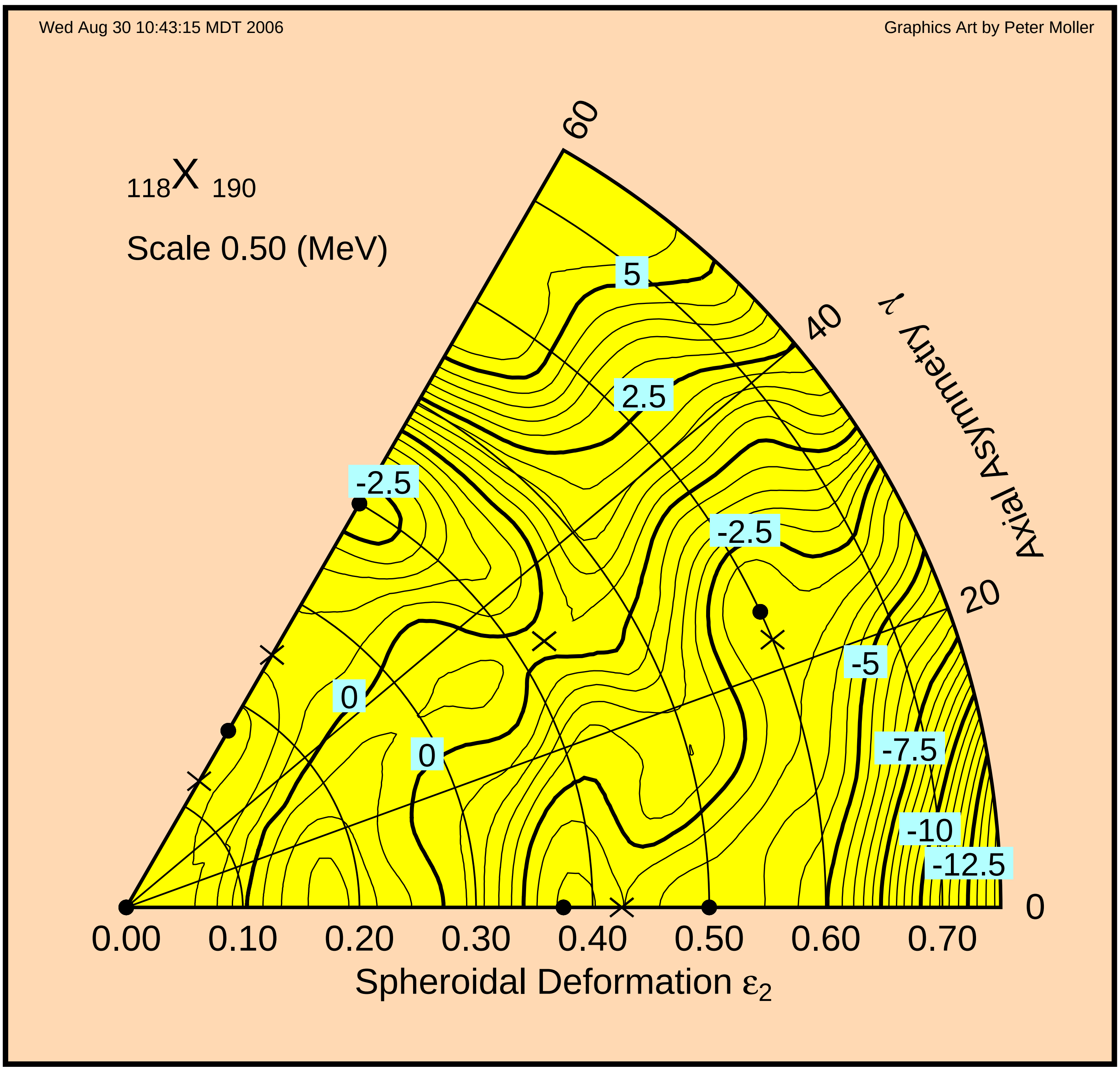

Wed Aug 30 10:43:15 MDT 2006
Graphics Art by Peter Moller
118X 190
Scale 0.50 (MeV)
60
40
20
0
Axial Asymmetry γ
5
2.5
-2.5
0
0
-2.5
-5
-7.5
-10
-12.5
0.00
0.10
0.20
0.30
0.40
0.50
0.60
0.70
Spheroidal Deformation ε2

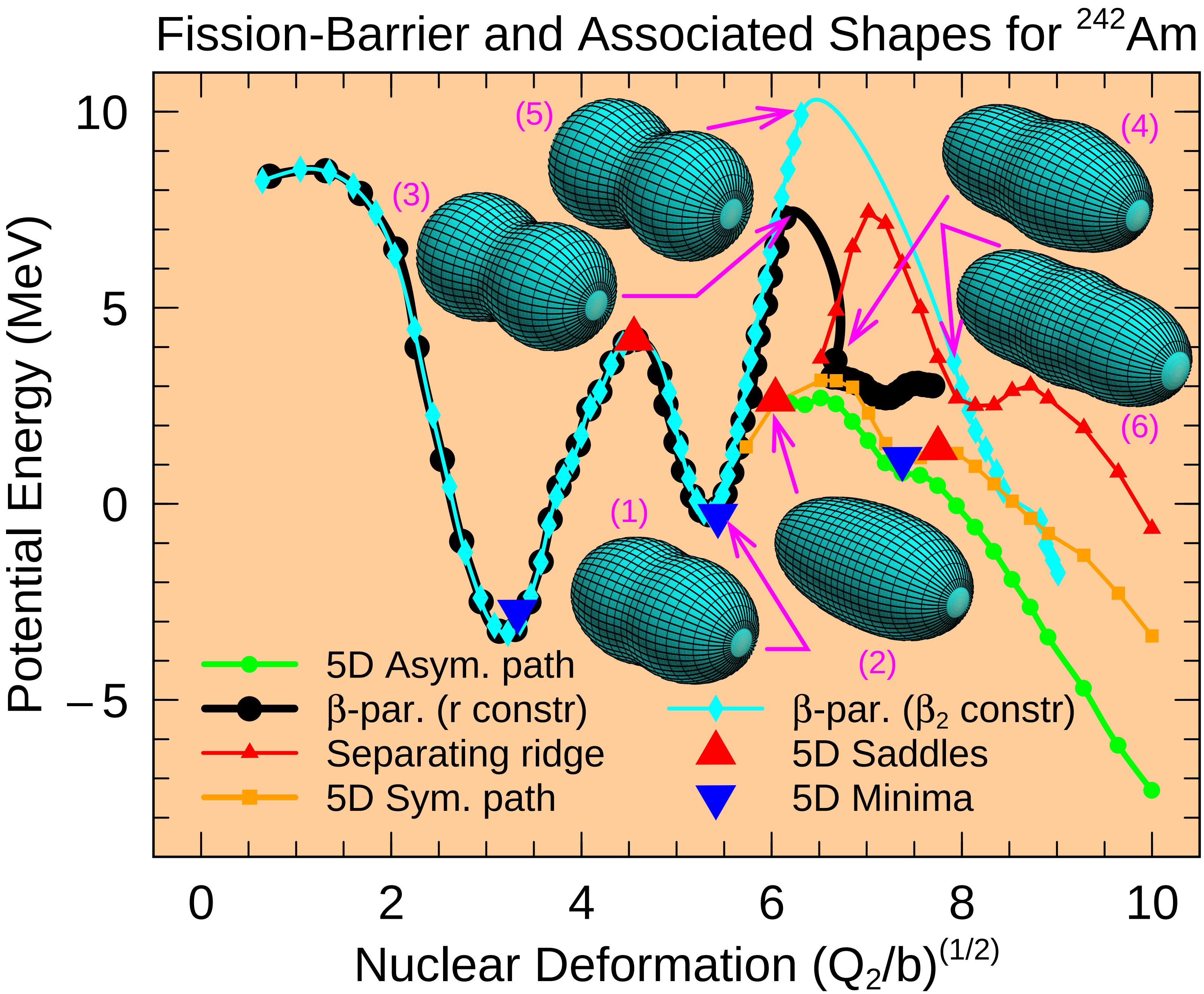

Fission-Barrier and Associated Shapes for ^{242}Am
Potential Energy (MeV)
Nuclear Deformation $(Q_2/b)^{(1/2)}$
10
5
0
−5
0
2
4
6
8
10
(1)
(2)
(3)
(4)
(5)
(6)
5D Asym. path
β-par. (r constr)
Separating ridge
5D Sym. path
β-par. (β_2 constr)
5D Saddles
5D Minima

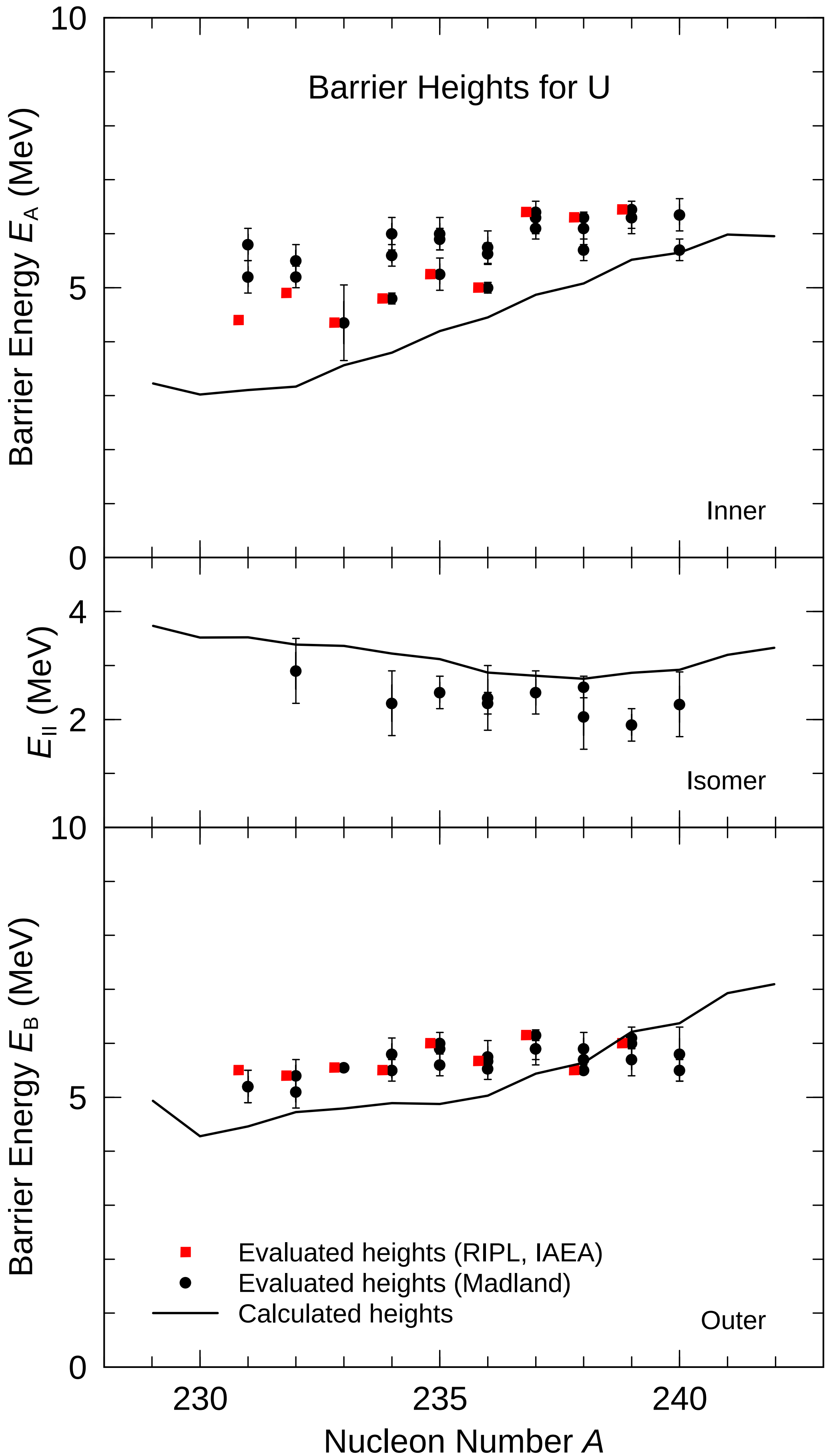

Barrier Heights for U
Barrier Energy E_A (MeV)
Inner
E_{II} (MeV)
Isomer
Barrier Energy E_B (MeV)
Outer
Evaluated heights (RIPL, IAEA)
Evaluated heights (Madland)
Calculated heights
Nucleon Number A
0
5
10
2
4
230
235
240

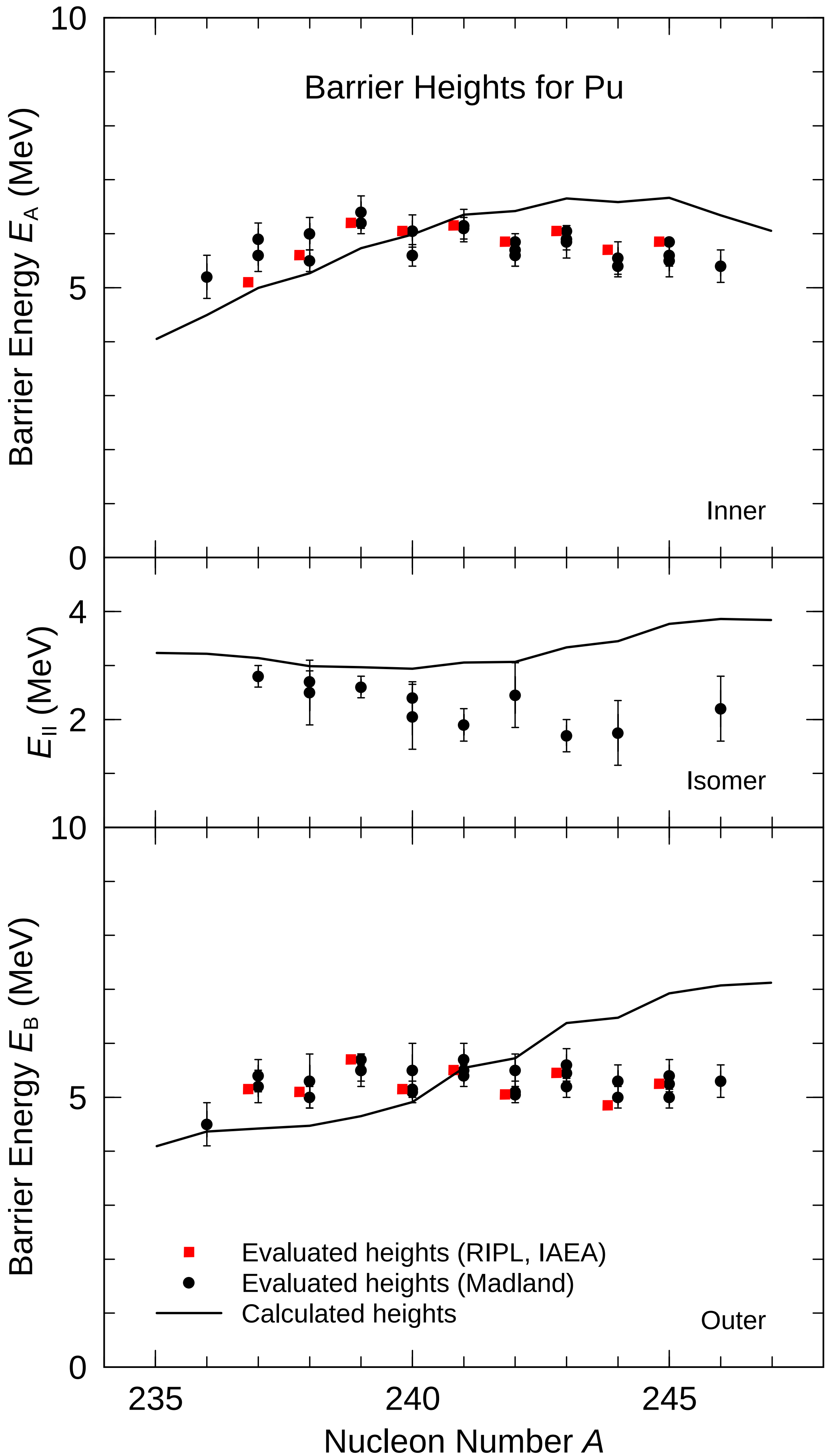

Barrier Heights for Pu
Barrier Energy E_A (MeV)
Inner
E_{II} (MeV)
Isomer
Barrier Energy E_B (MeV)
Outer
Evaluated heights (RIPL, IAEA)
Evaluated heights (Madland)
Calculated heights
Nucleon Number A
10
5
0
4
2
235
240
245

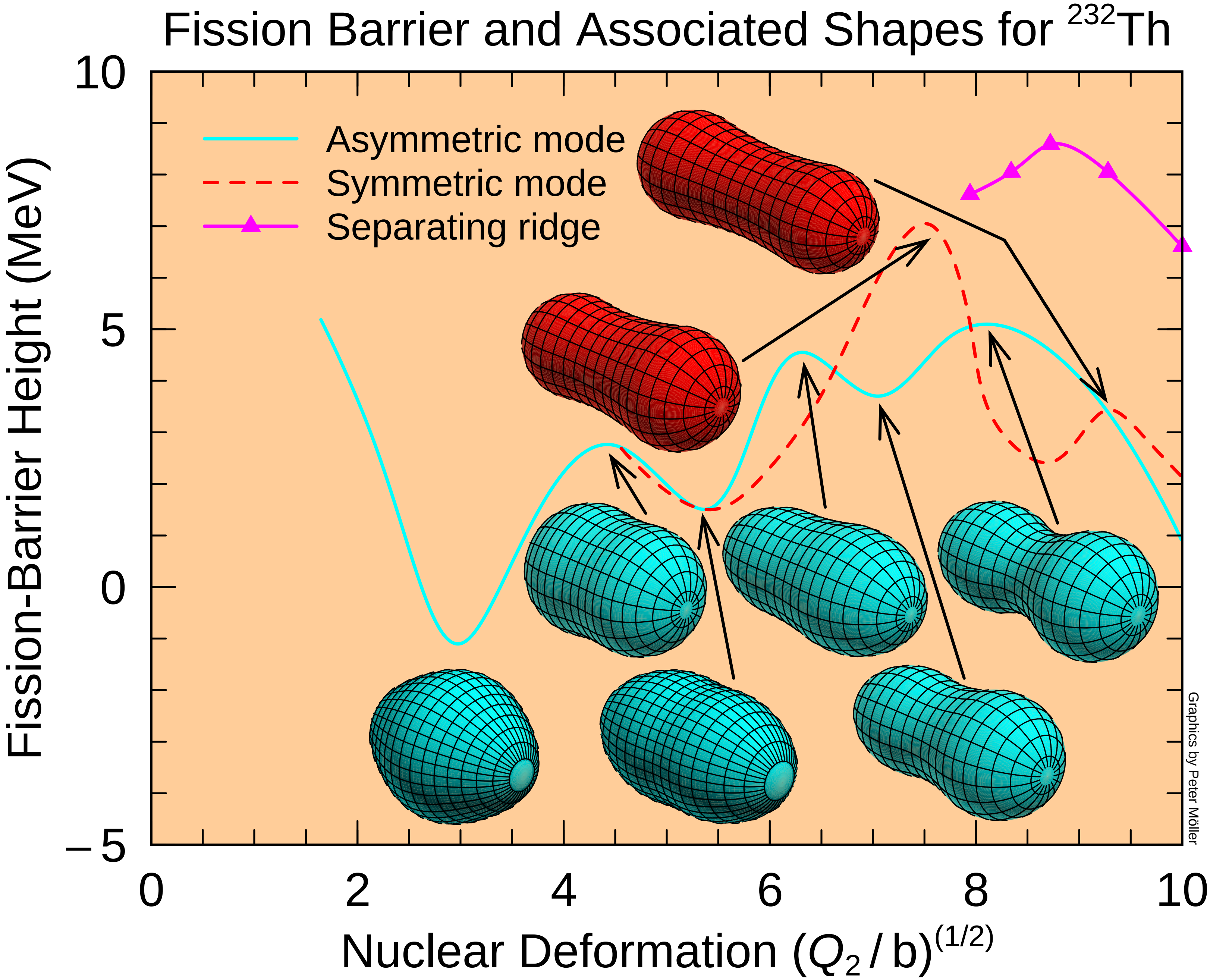

Fission Barrier and Associated Shapes for 232Th
Asymmetric mode
Symmetric mode
Separating ridge
Fission-Barrier Height (MeV)
10
5
0
−5
0
2
4
6
8
10
Nuclear Deformation (Q2 / b)(1/2)
Graphics by Peter Möller

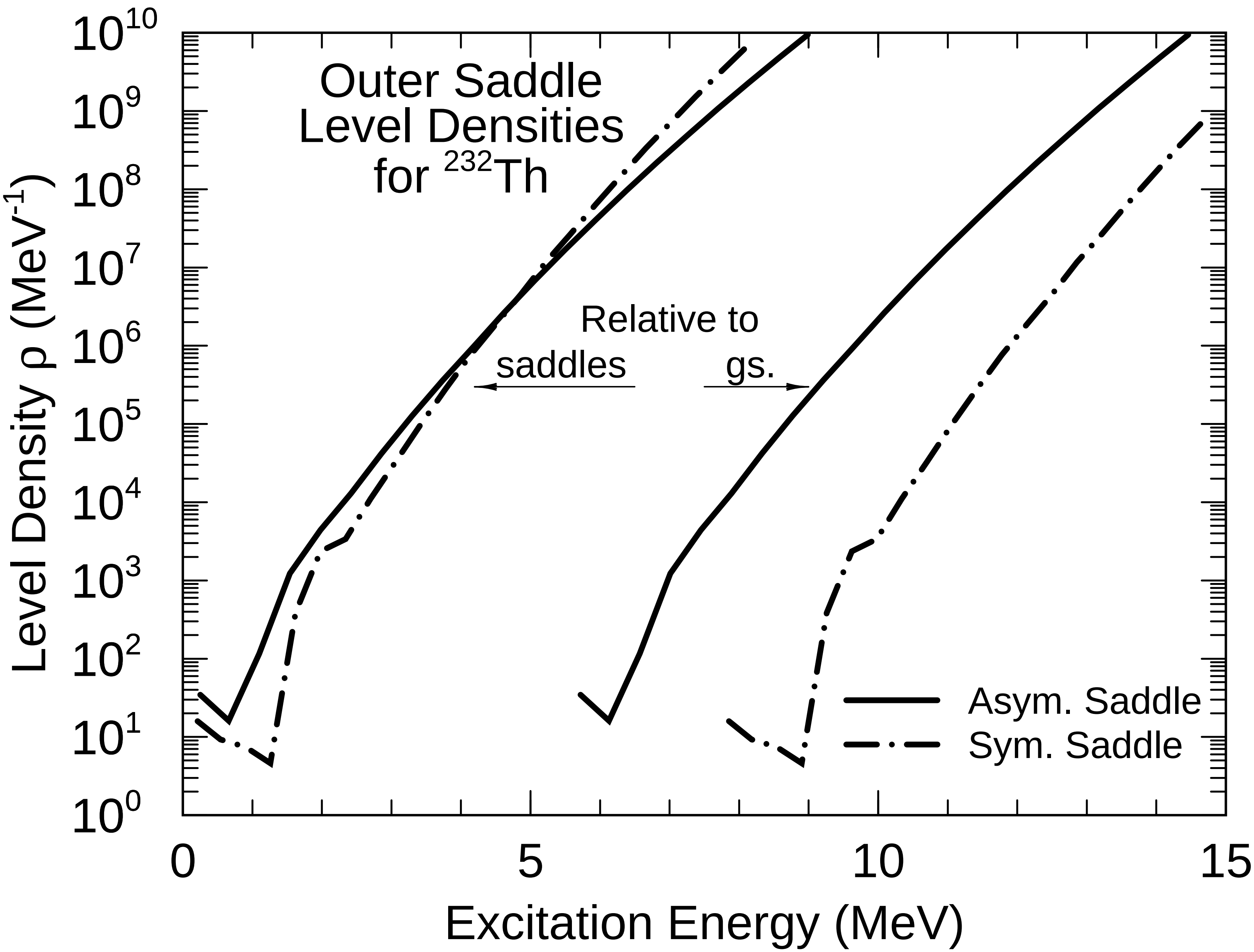

Outer Saddle
Level Densities
for 232Th
Relative to
saddles
gs.
Asym. Saddle
Sym. Saddle
Level Density ρ (MeV-1)
Excitation Energy (MeV)
10^0
10^1
10^2
10^3
10^4
10^5
10^6
10^7
10^8
10^9
10^10
0
5
10
15

TABLE I: Fermi-gas level-density parameters determined from adjustments of parameters of the Fermi-gas model to microscopic calculations of intrinsic level densities. The numbers in parentheses are (1) for an asymmetric saddle, and (2) for a symmetric saddle. B and C refer to the second and third saddle, respectively, for a triple-humped barrier, see Fig. **??**.

			Density Fit		Log Fit	
Nucleus		$Q_2^{1/2}$ (barn$^{1/2}$)	a (MeV)$^{-1}$	$E_{\rm shift}$ (MeV)	a (MeV)$^{-1}$	$E_{\rm shift}$ (MeV)
		even-even systems				
^{232}Th	(1)	7.75	17.708	2.483	15.403	1.177
^{232}Th	(2)	7.56	20.538	2.492	18.963	1.898
		odd-even systems				
^{239}Am	(1)	6.04	19.369	1.275	16.906	0.607
^{241}Am	(1)	6.04	19.879	1.232	19.156	0.980
^{243}Am	(1)	6.04	20.281	1.097	17.828	0.470
		odd-odd systems				
^{238}Am	(1B)	6.20	19.041	0.810	19.125	0.700
^{238}Am	(1C)	7.56	17.259	0.232	17.814	0.420
^{242}Am	(1)	6.04	19.740	0.618	21.961	0.980

Calculated Energy Window for EC-Delayed Fission

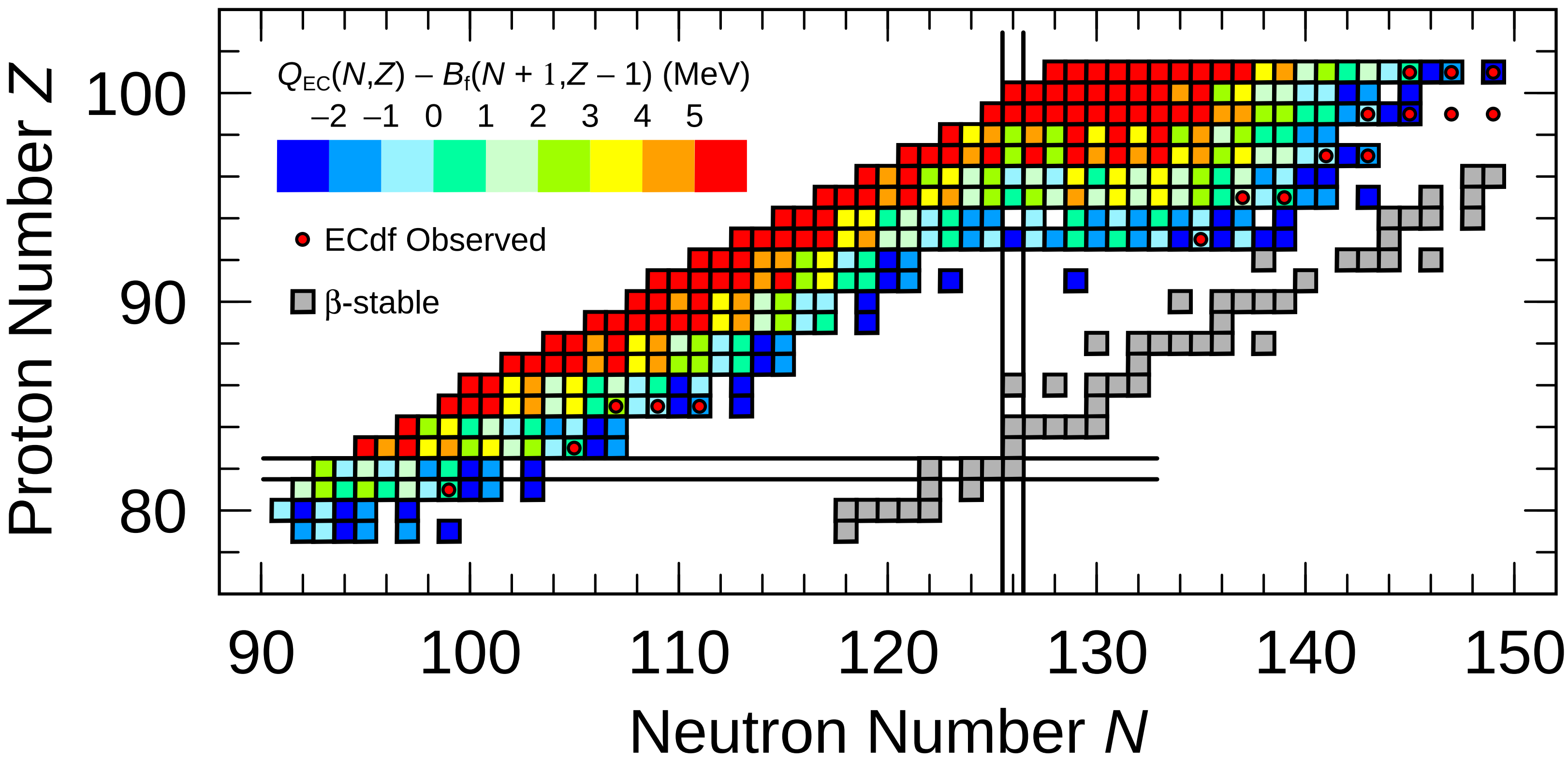

TABLE I: Calculated Q values Q_{EC} for electron capture and calculated fission-barrier heights B_{f} for reactions where EC-delayed fission has been observed experimentally.

Reaction	Q_{EC} (MeV)	B_{f} (MeV)	$Q_{\mathrm{EC}} - B_{\mathrm{f}}$ (MeV)
${}^{180}_{81}\mathrm{Tl} \stackrel{EC}{\Longrightarrow} {}^{180}_{80}\mathrm{Hg}$	10.44	9.81	0.63
${}^{228}_{93}\mathrm{Np} \stackrel{EC}{\Longrightarrow} {}^{228}_{92}\mathrm{U}$	4.26	5.13	−0.87
${}^{232}_{95}\mathrm{Am} \stackrel{EC}{\Longrightarrow} {}^{232}_{94}\mathrm{Pu}$	4.88	3.23	1.65
${}^{234}_{95}\mathrm{Am} \stackrel{EC}{\Longrightarrow} {}^{234}_{94}\mathrm{Pu}$	4.12	3.83	0.29
${}^{238}_{97}\mathrm{Bk} \stackrel{EC}{\Longrightarrow} {}^{238}_{96}\mathrm{Cm}$	4.77	4.92	−0.15
${}^{242}_{99}\mathrm{Es} \stackrel{EC}{\Longrightarrow} {}^{242}_{98}\mathrm{Cf}$	5.22	6.16	−0.94
${}^{244}_{99}\mathrm{Es} \stackrel{EC}{\Longrightarrow} {}^{244}_{98}\mathrm{Cf}$	4.45	6.69	−2.24
${}^{246}_{99}\mathrm{Es} \stackrel{EC}{\Longrightarrow} {}^{246}_{98}\mathrm{Cf}$	3.69	7.16	−3.47
${}^{248}_{99}\mathrm{Es} \stackrel{EC}{\Longrightarrow} {}^{248}_{98}\mathrm{Cf}$	2.98	7.24	−4.26

TABLE I: Fission and α-decay half-lives for selected nuclei. .

Nuclide			$^{10}\mathrm{Log}(T^{\mathrm{f}}_{1/2}/\mathrm{y})$		$^{10}\mathrm{Log}(T^{\alpha}_{1/2}/\mathrm{y})$	
Z	N	A	Calc.	Exp.	Calc.	Exp.
92	144	236	14.31	16.39	8.18	7.37
94	138	232	−1.29		−3.21	−4.19
94	146	240	9.22	11.05	4.51	3.93
100	152	252	6.06	2.09	−1.14	−2.54
100	158	258	−7.34	−10.91		
96	126	222	9.41		−4.12	
98	126	224	1.65		−4.70	
100	126	226	−3.03		−5.29	
96	128	224	−2.16		−8.35	
96	134	230	−10.76		−1.48	
98	132	230	−15.96		−4.52	
112	165	277	−5.37		−11.91	−11.11

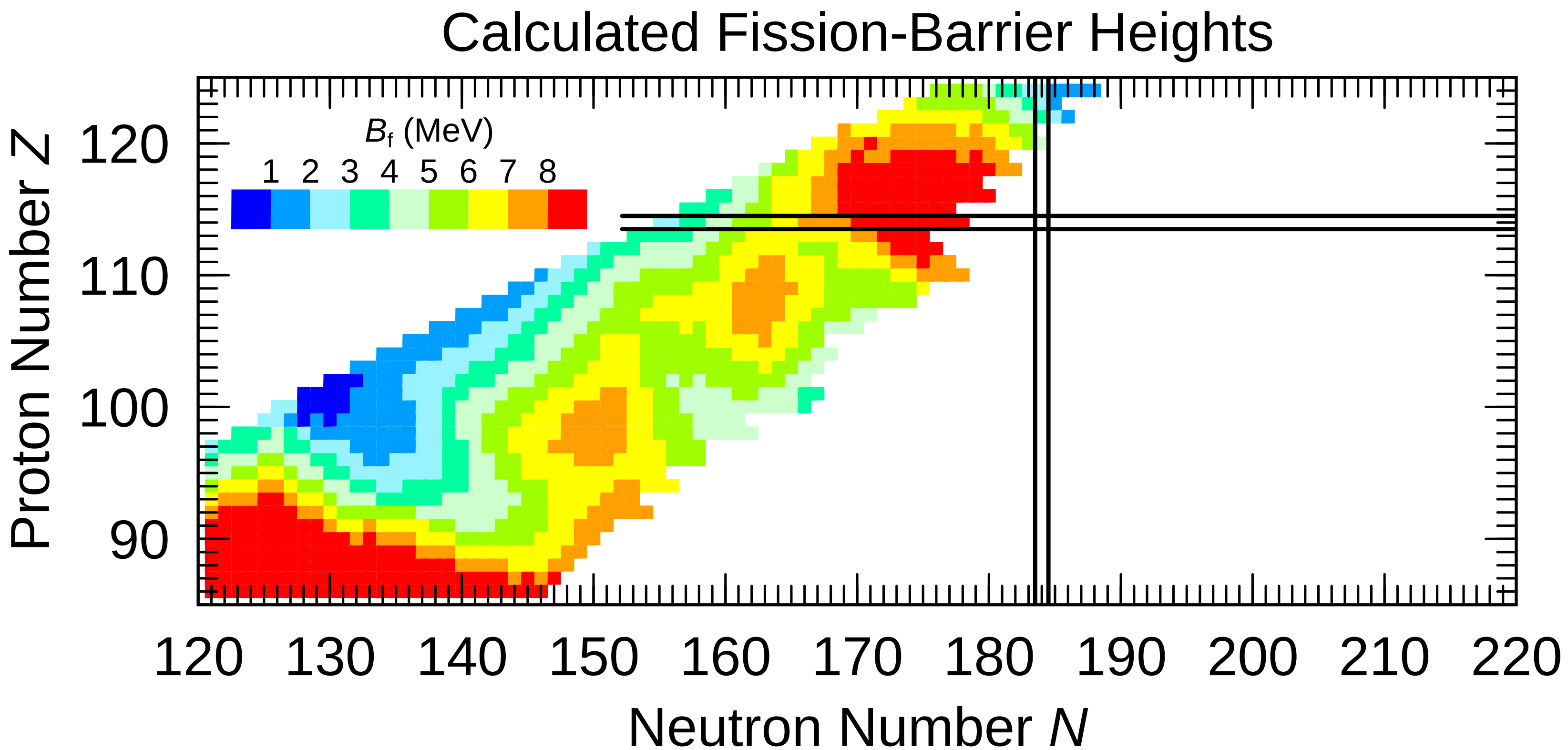

Calculated Fission-Barrier Heights
B_f (MeV)
1 2 3 4 5 6 7 8
Proton Number Z
120
110
100
90
120 130 140 150 160 170 180 190 200 210 220
Neutron Number N